1870 *Chem. Mater.* **2010,** *22,* 1870–1877
DOI:10.1021/cm903405s

CHEMISTRY OF MATERIALS
Article

Intercalation of Bulk Guest into LDH via Osmotic Swelling/Restoration Reaction: Control of the Arrangements of Thiacalix[4]arene Anion Intercalates

Gailing Huang,[†] Shulan Ma,[†] Xinhua Zhao,[†] Xiaojing Yang,*[,†] and Kenta Ooi[‡]

[†]*College of Chemistry, Beijing Normal University, Beijing 100875, China, and* [‡]*National Institute of Advanced Industrial Science and Technology, 2217-14 Hayashi, Takamatsu 761-0395, Japan*

Received November 6, 2009. Revised Manuscript Received December 23, 2009

Water-soluble tetrasodium *p*-sulfonatothiacalix[4]arene (TCAS) was intercalated into MgAl-LDH using an osmotic swelling/restoration reaction of the LDH in formamide. The restoration process was investigated in detail. The arrangement of TCAS in the interlayer can be controlled through adjusting the area per unit charge (S_{charge}) of TCAS. When S_{charge} (TCAS) < S_{charge} (LDH), monolayer (basal spacing, d_{basal}, 1.30 nm) and alternating "up-down" antiparallel (d_{basal}, 1.54 and 1.45 nm) arrangements were obtained. When S_{charge} of TCAS was increased by forming an Ag^+ complex, bilayer arrangement (d_{basal}, 2.12 nm) of TCAS(Ag) was formed. This swelling/restoration reaction took place, and the composites retained the morphology of the LDH precursor. The thermal stability of TCAS in the composites was remarkably enhanced, and the "up-down" antiparallel arrangement of TCAS had the highest increase of thermal stability.

Introduction

In the past 20 years, the organic/inorganic nanocomposites are a kind of the most promising materials, exhibiting a variety of unique properties due to the synergies of the inorganic and organic components.[1] Layered double hydroxides (LDHs), with the general formula $[M^{2+}_{1-y}M^{3+}_{y}(OH)_2][(X^{n-})_{y/n}\cdot mH_2O]$,[2] are a family of layered inorganic compounds consisting of stacks of positively charged metal hydroxide layers with anions in the interlayer, having been widely studied due to the characteristic of tunable composition and exchangeable anion in fields of catalysis,[3] separation science,[4,5] storage and triggered release of functional anions,[6,7] and optical materials.[8] For preparing the organic/LDH composite materials, traditional coprecipitation, ion exchange, and calcination-rehydration are the most common methods.[9−11] Through these methods, macrocyclic compounds such as calixarene,[12] crown ether,[13] cyclodextrin,[14] and porphyrin[15] were introduced into LDHs.

The delamination/restacking process is another way for synthesizing organic/LDH composites. Many negatively charged layered compounds, such as layered silicate,[16] perovskites,[17] titanium dioxides,[18] manganese oxide,[19]

*Corresponding author. Phone: +86-10-5880-2960. Fax: +86-10-5880-2075. E-mail: yang.xiaojing@bnu.edu.cn.

(1) (a) Innocenzi, P.; Brusatin, G. *Chem. Mater.* **2001**, *13*, 3126. (b) Ktov, N. V.; Magnov, S.; Tropsha, E. *Chem. Mater.* **1998**, *10*, 886. (c) Zhu, H. Y.; Lu, G. Q. *Langmuir* **2001**, *17*, 588.
(2) (a) Rudolf, A. *Acta Crystallogr., Sect. B: Struct. Sci.* **1968**, *24*, 972. (b) Braterman, P. S.; Xu, Z. P.; Yarberry, F.Layered Double Hydroxides (LDHs). In *Handbook of Layered Materials*; Auerbach, S. M., Carrado, K. A., Dutta, P. K.,Ed.; Marcel Dekker, Inc.: New York, 2004; p 373.
(3) (a) Cavani, F.; Trifiro, F.; Vaccari, A. *Catal. Today* **1991**, *11*, 173. (b) Sels, B.; De Vos, D.; Buntinx, M.; Pierard, F.; Kirsch-De Mesmaeker, A.; Jacobs, P. *Nature* **1999**, *400*, 855.
(4) (a) Pavan, P. C.; Gomes, G. De A.; Valim, J. B. *Microporous Mesoporous Mater.* **1998**, *21*, 659. (b) Pérez, M. R.; Pavlovic, I.; Barriga, C.; Cornejo, J.; Hermosín, M. C.; Ulibarri, M. A. *Appl. Clay. Sci.* **2006**, *32*, 245.
(5) Bish, D. L. *Bull. Mineral.* **1980**, *103*, 170.
(6) (a) Bonnet, S.; Forano, C.; de Roy, A.; Besse, J. P.; Maillard, P.; Momenteau, M. *Chem. Mater.* **1996**, *8*, 1962. (b) Tronto, J.; Sanchez, K. C.; Crepaldi, E. L.; Naal, Z. K.; Stanlei, I.; Valim, J. B. *J. Phys. Chem.* **2004**, *65*, 493.
(7) Geraud, E.; Prevot, V.; Forano, C.; Mousty, C. *Chem. Commun.* **2008**, 1554.
(8) Ogawa, M.; Kuroda, K. *Chem. Rev.* **1995**, *95*, 399.
(9) (a) Nicole, M.-D.; Julien, P.; Yaël, I.; Christine, T.-G.; Jean-Pierre, B.; Jean-Pierre, M. *J. Mater. Chem.* **2003**, *13*, 2582. (b) Jaubertie, C.; Holgado, M. J.; San Román, M. S.; Rives, V. *Chem. Mater.* **2006**, *18*, 3114. (c) Lee, J. H.; Rhee, S. W.; Jung, D. Y. *Chem. Commun.* **2003**, 2740.
(10) (a) Leroux, F.; Adachi-Pagano, M.; Intissar, M.; Chauviere, S.; Forano, C.; Besse, J.-P. *J. Mater. Chem.* **2001**, *11*, 105. (b) Singh, M.; Ogden, M. I.; Parkinson, G. M.; Buckley, C. E.; Connolly, J. *J. Mater. Chem.* **2004**, *14*, 871. (c) Adachi-Pagano, M.; Forano, C.; Besse, J.-P. *Chem. Commun.* **2000**, 91.
(11) Choy, J.-H.; Kwak, S.-Y.; Park, J.-S.; Jeong, Y.-J.; Portier, J. *J. Am. Chem. Soc.* **1999**, *121*, 1399.
(12) (a) Sasaki, S.; Aisawa, S.; Hirahara, H.; Sasaki, A.; Nakayama, H.; Narita, E. *J. Solid State Chem.* **2006**, *179*, 1129. (b) Sasaki, S.; Aisawa, S.; Hirahara, H.; Sasaki, A.; Nakayama, H.; Narita, E. *J. Eur. Ceram. Soc.* **2006**, *26*, 655.
(13) Ma, S.; Fan, C.; Du, L.; Huang, G.; Yang, X.; Tang, W.; Makita, Y.; Ooi, K. *Chem. Mater.* **2009**, *21*, 3602.
(14) (a) Zhao, H.; Vance, G. F. *J. Chem. Soc., Dalton Trans.* **1997**, 1961. (b) Sasaki, S.; Yokohama, Y.; Aisawa, S.; Hirahara, H.; Narita, E. *Chem. Lett.* **2005**, *34*, 1192.
(15) Bonnet, S.; Forano, C.; De Roy, A.; Besse, J. P.; Momenteau, M. *Chem. Mater.* **1996**, *8*, 1962.
(16) (a) Lerf, A.; Schöllhorn, R. *Inorg. Chem.* **1977**, *16*, 2950. (b) Nadeau, P. H.; Wilson, M. J.; McHardy, W. J.; Tait, J. M. *Science* **1984**, *225*, 923. (c) Strawhecker, K. E.; Manias, E. *Chem. Mater.* **2000**, *12*, 2943.
(17) Schaak, R. E.; Mallouk, T. E. *Chem. Mater.* **2002**, *14*, 1455.
(18) Sasaki, T.; Watanabe, M. *J. Am. Chem. Soc.* **1998**, *120*, 4682.

Published on Web 01/11/2010

zirconium phosphate,[20] and oxovanadium phosphate,[21] can be delaminated into unilaminar nanosheets. The nanosheets could be utilized as building block for bottom-up assembly with organic molecules or ions to prepare nanocomposites. To obtain positively charged nanosheets, the delamination of LDHs has been extensively studied.[22] Recently, it has been found that formamide[23] is a simple and effective solvent for delaminating LDHs at room temperature. Utilizing the LDH nanosheets, CdSe nanoparticles[24] and polymer (cellulose)[25] were introduced into LDHs via a costacking process, and core−shell materials and multilayer films were synthesized via the layer-by-layer technique.[23b,26]

Swelling is a prelude before delamination, including a short-range swelling and osmotic swelling.[27] The Sasaki group investigated the delamination process of LDHs in formamide and pointed out[28] that (1) delamination follows two separate processes: rapid swelling and subsequent slow exfoliation and (2) the swelling phase, only with mechanical shearing or ultrasonic, could achieve successful delamination. The osmotic swelling provides an open space for bulky anions to introduce into; however, there is a lack of study focusing on it. We have communicated that TCAS (water-soluble tetrasodium *p*-sulfonatothiacalix[4]arene) can be introduced into the osmotically swollen LDH phase, leading to the recovery of the sheets.[29] This exhibits that the osmotic swelling/restoration process provides an alternative to the existing ways for preparing composites.

In this paper, we investigate, in detail, the preparation of the TCAS/LDH nanocomposites via the osmotic swelling/restoration reaction. The monolayered, bilayered, and alternating "up-down" antiparallel arrangements of TCAS in the interlayer of the restored composites were obtained. In the viewpoint of applications, the present preparation method provides novel secondary-host materials with a controllable structure for specific secondary host−guest reactions.

Experimental Section

TCAS and TCAS-Ag Complex. *p-tert*-Butylthiacalix[4]arene (TCA) was prepared according to the literature.[30] The sulfonation of TCA was carried out as follows.[31] TCA (1.75 g) was added to 80 mL of concentrated sulfuric acid, and the suspension was heated at 80 °C for 4 h. After having been cooled, the mixture was poured into ice−water (500 mL), and NaCl (100 g) was added to salt out sodium salt. The purple solid residue was filtered and dissolved in minimum water, and then 4-fold ethanol was poured to give a white precipitate. By repeating this procedure four times, pure TCAS (1.2 g) was obtained.

In order to decrease the charge number of TCAS, we tried to decrease the deprotonation degree by adding HCl, but it was unsuccessful because of the weak acid resistance of the LDH layer. Thus, the TCAS−Ag complex was used. The TCAS−Ag complex was prepared according to the literature.[32] TCAS (0.11 g) was dissolved in a little deionized water. The $AgNO_3$ solution (5 mL, 20 mM) was taken out from the volumetric flask by transfer pipet and then dropped into the TCAS solution with stirring. The mixture solution was stirred for 2 h at room temperature, and the color turned light brown.

Osmotic Swelling of NO_3^-−LDH. Highly crystallized MgAl−CO_3^{2-}−LDH was synthesized through the urea hydrolysis method.[33] A mixed solution containing $Mg(NO_3)_2$ (0.1 M), $Al(NO_3)_3$ (0.05 M), and urea (0.245 M) was hydrothermally treated at 140 °C for 24 h in a Teflon-autoclave. The precipitate was filtered, washed, and then dried at 70 °C. The NO_3^-−LDH was prepared through NO_3^-/CO_3^{2-} ion-exchange reaction by putting the CO_3^{2-}−LDH crystals (1 g) in a solution (1000 mL) of HNO_3 (5 mM) and $NaNO_3$ (1 M),[34] sonicated for 20 min and filtered.

To prepare LDH nanosheets in an osmotic swelling state, the NO_3^-−LDH crystals (0.075 g) were added to 30 mL of formamide, and then the mixture was allowed to stand for 24 h *without stirring or shaking*. A translucent colloidal suspension was obtained.

Restoration of the Swollen LDH Nanosheets with TCAS. Weighed TCAS (from 0.01 to 0.15 g) was put into the prepared colloidal suspension of the LDH in formamide and stirred slowly for 24 h. After having been centrifuged at 18000 rpm, the obtained slurry was washed several times with degassed water (40 mL each time). Finally, the obtained solid was air-dried at room temperature.

TCAS (0.15 g) was dissolved in about 5 mL of distilled water, and then 0.027 g of NaOH (the molar ratio of NaOH /TCAS is about 4) was added into the solution for adjusting the charge of TCAS. Finally, the mixture solution was added into the colloidal suspension. The restored composite was noted as RC−0.15−NaOH.

Using the same method, the prepared TCAS−Ag complex solution (5 mL) was poured into the colloidal suspension of the LDH. The obtained composite was noted as RC−Ag (0.11 g of TCAS).

Characterization Technique. The powder X-ray diffraction (XRD) patterns were collected using a Phillips X' pert Pro MPD diffractometer with $Cu-K_\alpha$ radiation. The generator setting is

(19) (a) Liu, Z.-h.; Ooi, K.; Kanoh, H.; Tang, W.; Tomida, T. *Langmuir* **2000**, *16*, 4154. (b) Omomo, Y.; Sasaki, T.; Wang, L.; Watanabe, M. *J. Am. Chem. Soc.* **2003**, *125*, 3568.
(20) Alberti, G.; Casciola, M.; Costantino, U.; Di Gregorio, F. *Solid State Ionics* **1989**, *32*, 40.
(21) (a) Yamamoto, N.; Okuhara, T.; Nakato, T. *J. Mater. Chem.* **2001**, *11*, 1858. (b) Kamiya, Y.; Yamamoto, N.; Imai, H.; Komai, S.; Okuhara, T. *Microporous Mesoporous Mater.* **2005**, *81*, 49.
(22) (a) Jobbágy, M.; Regazzoni, A. E. *J. Colloid Interface Sci.* **2004**, *275*, 345. (b) ÓLeary, S.; ÓHare, D.; Seeley, G. *Chem. Commun.* **2002**, 1506. (c) Hibino, T.; Jones, W. *J. Mater. Chem.* **2001**, *11*, 1321. (d) Hibino, T.; Kobayashi, M. *J. Mater. Chem.* **2005**, *15*, 653.
(23) (a) Hibino, T. *Chem. Mater.* **2004**, *16*, 5482. (b) Liu, Z.; Ma, R.; Osada, M.; Iyi, N.; Ebina, Y.; Takada, K.; Sasaki, T. *J. Am. Chem. Soc.* **2006**, *128*, 4872. (c) Liu, Z. P.; Ma, R. Z.; Ebina, Y.; Iyi, N.; Takada, K.; Sasaki, T. *Langmuir* **2007**, *23*, 861.
(24) Venugopal, B. R.; Ravishankar, N.; Perrey, C. R.; Shivakumara, C.; Rajamathi, M. *J. Phys. Chem. B* **2006**, *110*, 772.
(25) Kang, H.; Huang, G.; Ma, S.; Bai, Y.; Ma, H.; Li, Y.; Yang, X. *J. Phys. Chem. C.* **2009**, *113*, 9157.
(26) (a) Li, L.; Ma, R. Z.; Iyi, N.; Ebina, Y.; Takada, K.; Sasaki, T. *Chem. Commun.* **2006**, 3125. (b) Li, L.; Ma, R. Z.; Ebina, Y.; Fukuda, K.; Takada, K.; Sasaki, T. *J. Am. Chem. Soc.* **2007**, *129*, 8000. (c) Li, L.; Ma, R.; Ebina, Y.; Iyi, N.; Sasaki, T. *Chem. Mater.* **2005**, *17*, 4386.
(27) Sasaki, T.; Watanabe, M. *J. Am. Chem. Soc.* **1998**, *120*, 4682.
(28) Ma, R.; Liu, Z.; Li, L.; Iyi, N.; Sasaki, T. *J. Mater. Chem.* **2006**, *16*, 3809.
(29) Huang, G.; Ma, S. L.; Zhao, X. H.; Yang, X.; Ooi, K. *Chem. Commun.* **2009**, 331.
(30) Iyi, N.; Fujimoto, T.; Miyano, S. *Chem. Lett.* **1998**, 625.
(31) Yuan, D. Q.; Zhu, W. X.; Ma, S. L.; Yan, X. *J. Mol. Struct.* **2002**, *616*, 241.
(32) Yuan, D. Q. Master's thesis/doctoral dissertation, Beijing Normal University, **2002**.
(33) Okamoto, K.; Iyi, N.; Sasaki, T. *Appl. Clay Sci.* **2007**, *37*, 23.
(34) Iyi, N.; Matsumoto, T.; Kaneko, Y.; Kitamura, K. *Chem. Mater.* **2004**, *16*, 2926.

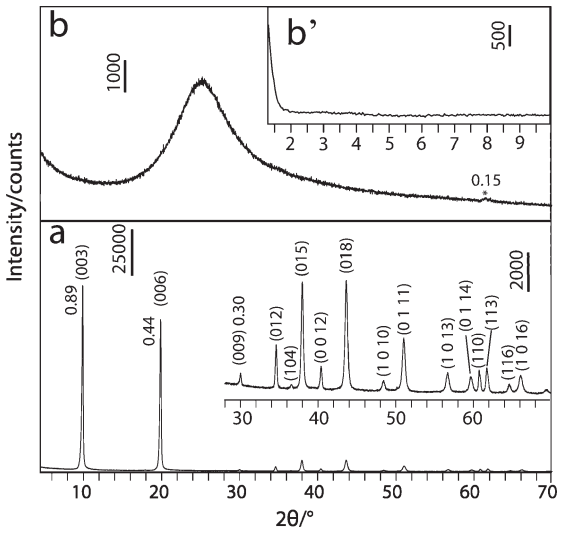

Figure 1. XRD patterns of the samples (a) MgAl−NO_3^- −LDH and (b, b') wet colloidal aggregate of NO_3 −LDH in formamide. *d*-value in nanometers.

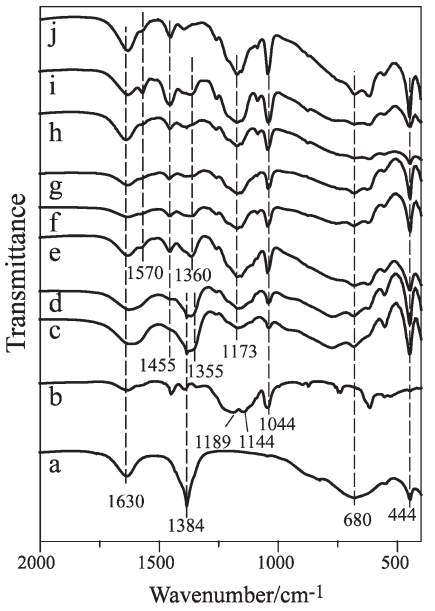

Figure 2. The FTIR spectra of (a) NO_3^- −LDH, (b) TCAS, and the restored samples (c) RC−0.01, (d) RC−0.02, (e) RC−0.04, (f) RC−0.05, (g) RC−0.075, (h) RC−0.15, (i) RC−Ag, and (j) RC−0.15−NaOH.

40 kV and 40 mA. The XRD patterns were measured at room temperature with step size of 0.017° and a scan time of 10 s per step. For the small degrees, the XRD patterns were measured at room temperature with a step size of 0.008° and a scan time of 30 s per step. Fourier-transform Infrared (FT-IR) spectra of the samples were recorded on a Nicolet-380 Fourier-transform infrared spectrometer using the KBr method in the range of 400−4000 cm^{-1}. Scanning electron microscope (SEM) observation was carried out using a mode S-4800 (Hitachi, Ltd.) operating at 5.0 kV.

The C, H, and N contents were analyzed on a LECO CS-444 analyzer, while the contents of Mg, Al, S, and Ag were determined by inductively coupled plasma (ICP) atomic emission spectroscopy (Jarrel-ASH, ICAP-9000) after the samples (13−15 mg) were dissolved in 4 mL of concentrated nitric acid and then diluted to 100 mL.

Thermal gravimetric (TG) and differential scanning calorimeters (DSC) data were collected using a NETZSCH STA 409 PC/PG thermal analyzer. The sample was put into alumina crucible, and the heating rate was 10 °C/min.

Results and Discussion

Characteristic of LDH Osmotic Swelling Phase. Figure 1a is the XRD pattern of the MgAl−NO_3^-−LDH crystals. All the peaks can be indexed to a hexagonal symmetry with lattice parameters a = 0.30475(5) and c = 2.6776(4) nm. The basal spacing (d_{basal}) of 0.89 nm showed the interlayer of NO_3^- species, which was testified by the IR adsorption band at 1385 cm^{-1} (Figure 2a).[35] The NO_3^-−LDH crystals had a shape of hexagonal platelets with a size of ~2 μm across the hexagonal surface (Figure 3a), well retaining the morphology of the CO_3^{2-}−LDH precursor.

The colloidal suspension obtained by adding the NO_3^-−LDH crystals into formamide had a Tyndall light scattering (Figure S1a, Supporting Information). After having been centrifuged, the colloidal aggregate showed a

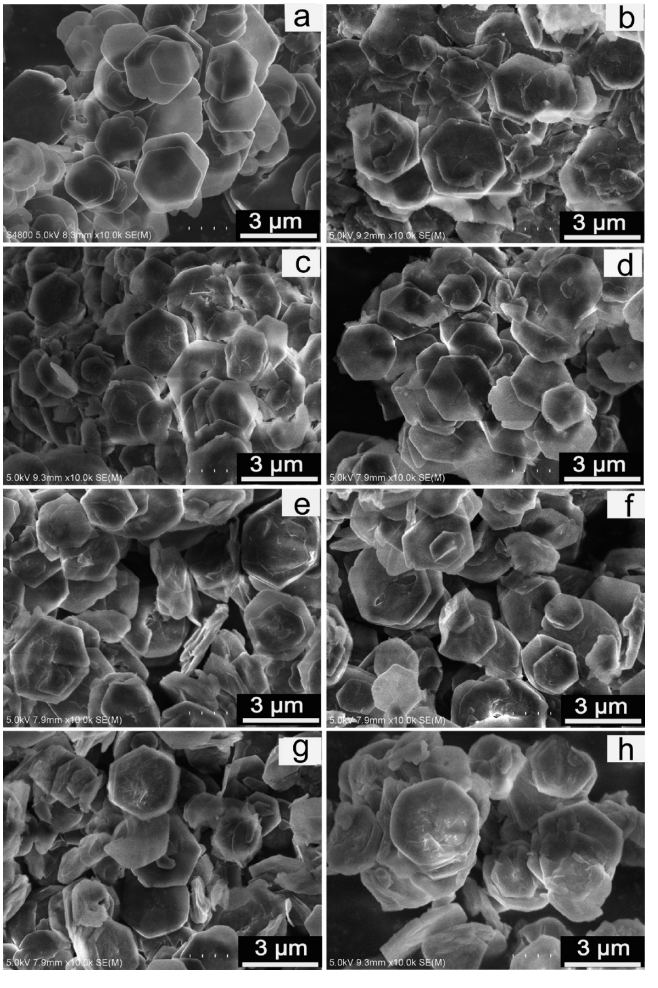

Figure 3. SEM images of (a) MgAl−NO_3^-−LDH crystals and the restored samples (b) RC−0.01, (c) RC−0.02, (d) RC−0.04, (e) RC−0.05, (f) RC-0.075, (g) RC−0.15, and (h) RC−Ag.

XRD pattern (Figure 1b) with a halo in 2θ range of 20−30°, attributed to liquid formamide,[23b,26c,29] and a

(35) Wu, Q.; Olafsen, A.; Vistad, O. B.; Roots, J.; Norby, P. *J. Mater. Chem.* **2005**, *15*, 4695.

small peak at the d value of 0.15 nm. The peak corresponds to the (110) plane of the LDH, indicating the existence of hydroxide sheets as two-dimensional crystals. In the low degree range (Figure 1b'), there was no peak or halo, as we reported previously, indicating that the nanosheets are in an osmotic swelling state[29] with a distance larger than 8.8 nm ($2\theta = 1°$). Such a diffraction feature is the same as reported by Liu et al. in a 0.1 g CoAl−LDH/0.5 cm^3 formamide system, for which they considered that a swollen phase with a very large gallery height might form.[23b] We consider that the swelling can be spontaneous,[36] that is, the layered structure extends to full the volume of the solution due to the strong repulsion at layer surfaces, so the expansion ratio of LDH layers can be evaluated from the equation, $V_f/V_{LDH} = V_f/(W_{LDH}/\rho_{LDH})$, where V_f and V_{LDH} are the volumes of formamide and the LDH, respectively, and W_{LDH} and ρ_{LDH} are the weight and density (about 2.0 $g\cdot cm^{-3}$) of the LDH, respectively. At the present experimental condition, the expansion ratio is 800 (30 cm^3/(0.075 g/2.0 $g\cdot cm^{-3}$)). This ratio maybe leads to a highly swelling interlayer distance of ca. 710 nm (800 × 0.89 nm, in which 0.89 nm is the d_{basal} of NO_3^-−LDH). For a swollen LDH phase in formamide, Sasaki et al. also considered that a large gallery height with several hundreds of nanometers might form.[28]

Formation of the Structure of Monolayered TCAS in the Interlayer. When the TCAS was added into the colloidal solution of the LDH in formamide, the solution became cloudy and the Tyndall phenomenon disappeared (Figure S1b). After having been water-washed and dried, the restored samples were obtained, noted as RC−x, where x is the amount of TCAS, 0.01, 0.02, 0.04, 0.05, 0.075, and 0.15 g, respectively. The products were yellow for RC−0.01 and RC−0.02 and white for the other samples with high TCAS contents. The XRD patterns (Figure 4) indicate that the samples had layered structures with two kinds of basal spacings (d_{basal}), 1.30 and 1.54 nm. Table 1 shows their compositions. The Mg/Al molar ratio was hardly changed after the swelling/restoration process. The 1.30 nm d_{basal} corresponds to TCAS contents lower than 0.04 per $Mg_{0.67}Al_{0.33}(OH)_2$ formula, while the larger d_{basal} value of 1.54 nm, to the contents higher than 0.04. RC−0.04 exhibited both the layer distances of 1.3 and 1.54 nm (Figure 4c). The least TCAS content introduced in RC−0.01 gave a separated NO_3^-−LDH phase shown by a d_{basal} of 0.88 nm as a main phase, besides the minor phase of TCAS intercalated (1.3 nm d_{basal}). The separated NO_3^- intercalated phase disappeared when the TCAS content increased (RC−0.02), and the 1.30 nm phase shown by the peaks of 1.30, 0.65, and 0.43 nm became dominant, accompanying with the separated CO_3^{2-} phase (the peaks of 0.76 and 0.38 nm). With an increase of TCAS content, $CO_3^{2-} + NO_3^-$ contents were decreased (Table 1). These results show that the TCAS anion with −6 charge has a strong affinity with the positively−charged LDH nanosheet, comparable to or stronger than CO_3^{2-}.

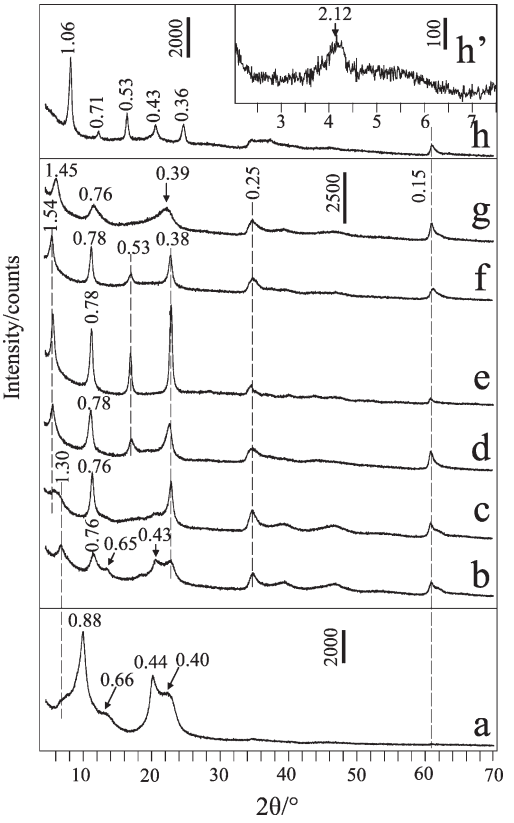

Figure 4. XRD patterns of the restored samples (a) RC−0.01, (b) RC−0.02, (c) RC−0.04, (d) RC−0.05, (e) RC−0.075, (f) RC−0.15, (g) RC−0.15−NaOH, and (h) RC−Ag. d-value in nanometers.

The SEM images (Figure 3) of the samples exhibited the well-recovered hexagonal platelets, i.e. the restored crystals had the same morphology as the precursor. The recovery of the morphology was hardly obtained by a delamination/restacking process.[37] Thus, the morphology recovery can be the evidence that the colloidal LDH nanosheets were in an osmotic swelling state rather than a delamination one. These results indicate that the introduction of TCAS leads to recovery of the swollen nanosheets.

The XRD patterns of the samples before and after water-washing indicate that the layered structures were formed after TCAS was added in formamide, and the d_{basal} values decreased by 0.3 nm for RC−0.02 (Figure 5a-a") and 0.2 nm for RC−0.15 (Figure 5b-b"). The decreases are due to the removal of formamide, as proved by the disappearance of 1690 cm^{-1} (C=O vibration of formamide) in FT−IR spectra (Supporting Information, Figure S2).

The structure of TCAS is shown in Scheme 1. Four benzene groups are connected by S bridges forming a hollow, and four SO_3^- groups in the upper-rim and two phenolate groups in the bottom-rim give −6 charges. The height of the molecule is estimated as to ~0.6 nm, and the diameters of the upper-rim and bottom-rim are ~1.1 and 0.5 nm, respectively.[31] Because the thickness of the LDH layer is 0.48 nm,[38] the gallery height of the restored

(36) Israelachvili, J. N. *Intermolecular and Surface Forces*, 2nd ed.; Academic Press Ltd.: London, 1991; p 248.
(37) Yang, X.; Makita, Y.; Liu, Z.-H.; Sakane, K.; Ooi, K. *Chem. Mater.* **2004**, *16*, 5581.
(38) Miyata, S. *Clays Clay Miner.* **1975**, *23*, 369.

Table 1. Chemical Analysis and the Formula of the Restored Samples

sample	content calculated (found) /wt%							$\frac{Mg}{Al}$	formula (TCAS = $C_{12}H_{10}O_{16}S_8$)	d_{basal}/ nm
	Mg	Al	Ag	S	C	H	N			
NO_3^-−LDH	19.17 (20.34)	10.47 (11.11)			0.18 (0.19)	3.36 (4.0)	5.02 (4.93)	2.04	$Mg_{0.67}Al_{0.33}(OH)_2(NO_3)_{0.30}(CO_3)_{0.01}\cdot 0.3H_2O$	0.89
RC−0.01	17.77 (16.86)	10.31 (9.78)		3.75 (3.55)	5.64 (5.25)	4.08 (3.87)	0.60 (0.57)	1.92	$Mg_{0.66}Al_{0.34}(OH)_2(TCAS)_{0.013}(CO_3)_{0.11}(NO_3)_{0.038}\cdot 0.8H_2O$	1.30, 0.88
RC−0.02	16.44 (15.45)	9.11 (8.56)		6.35 (5.97)	8.15 (7.30)	3.98 (3.74)	0.26 (0.24)	2.01	$Mg_{0.67}Al_{0.33}(OH)_2(TCAS)_{0.024}(CO_3)_{0.083}(NO_3)_{0.018}\cdot 0.8H_2O$	1.30, 0.76
RC−0.04	14.42 (13.71)	8.22 (7.81)		9.08 (8.63)	10.71 (10.45)	3.96 (3.76)		1.95	$Mg_{0.66}Al_{0.34}(OH)_2(TCAS)_{0.039}(CO_3)_{0.047}\cdot 1.0H_2O$	1.30, 0.76, 1.54
RC−0.05	13.98 (13.68)	7.37 (7.22)		10.82 (10.59)	12.33 (12.93)	3.85 (3.77)		2.11	$Mg_{0.68}Al_{0.32}(OH)_2(TCAS)_{0.050}(CO_3)_{0.016}\cdot 1.0H_2O$	1.54
RC−0.075	13.40 (12.77)	7.35 (7.01)		10.17 (9.69)	11.64 (11.66)	4.13 (3.94)		2.03	$Mg_{0.67}Al_{0.33}(OH)_2(TCAS)_{0.050}(CO_3)_{0.015}\cdot 1.2H_2O$	1.54
RC−0.15	13.26 (12.94)	7.60 (7.41)		11.73 (11.44)	13.19 (12.78)	3.76 (3.66)		1.94	$Mg_{0.66}Al_{0.34}(OH)_2(TCAS)_{0.055}\cdot 0.9H_2O$	1.54
RC−Ag	10.49 (10.14)	5.77 (5.58)	6.27 (6.28)	9.30 (9.00)	11.24 (11.12)	4.21 (4.07)		2.02	$Mg_{0.67}Al_{0.33}(OH)_2(TCAS)_{0.056}Ag_{0.093}(CO_3)_{0.10}\cdot 1.9H_2O$	2.12
RC−0.15−NaOH	13.65 (13.57)	7.90 (7.76)		11.03 (10.49)	12.40 (12.76)	3.74 (3.75)		1.96	$Mg_{0.66}Al_{0.34}(OH)_2(TCAS)_{0.050}\cdot 0.92H_2O$	1.45

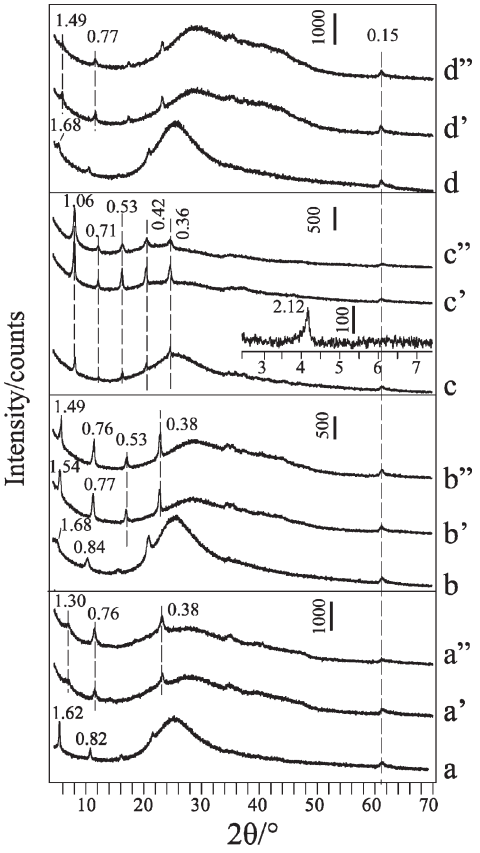

Figure 5. The XRD patterns of the unwashed restored samples (a) RC−0.02, (b) RC−0.15, (c) RC−Ag, and (d) RC−0.15−NaOH and the corresponding samples water-washed 1 and 4 times, respectively. *d*-value in nanometers.

Scheme 1. Schematic Structure and Dimensions of TCAS

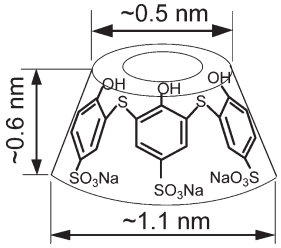

products with d_{basal} of 1.3 nm can be calculated as ~0.80 nm (1.30−0.48), close to the height of TCAS of 0.60 nm. The 1.3 nm d_{basal} with a TCAS orientation vertical to the layer agrees well with the result (1.33 nm) reported by Sasaki et al.[12] using a coprecipitation method to intercalate traditional calixarene (no S bridges). The slightly larger d_{basal} value of 1.54 nm indicates that the TCAS molecules take an alternating "up-down" antiparallel arrangement.[29] Further increase of TCAS added did not change the d_{basal} value, implying that the gallery structure is stable. The gallery distance of 1.06 nm (1.54 nm−0.48 nm) coincides well with that (~1 nm) estimated from the crystal data of TCAS.[31] This claylike arrangement of TCAS was observed in the pure TCAS[31] and traditional calixarene crystals.[39]

(39) Orr, G. W.; Barbour, L. J.; Atwood, J. L. *Science* **1999**, *285*, 1049.

When NaOH was added, the sample (noted as RC−0.15−NaOH) showed a basal spacing of 1.45 nm, implying a similar gallery structure to the 1.54 phase. But the slightly less d_{basal} indicates the strong interaction between the layers and TCAS with a high negative charge (−7). The negative charge was determined by the composition analysis, agreeing with the higher deprotonation extent in a stronger alkaline environment.

The area per unit charge (S_{charge}) is usually used to explain the structure obtained by an intercalation reaction.[13,40] The S_{charge} values for LDH layers and $TCAS^{6-}$, calculated from the crystal parameter a of NO_3^-−LDH and the upper-rim diameter ($D \approx 1.1$ nm) of $TCAS^{6-}$, are $3a^2 \cdot \sin 60° = 0.24$ nm^2 and $(D^2 \cdot \pi/4)/6 = 0.16$ nm^2, respectively. The latter is smaller than the former, so a monolayer arrangement[40,41] should be formed. The much smaller S_{charge} value (0.14 nm^2) for the RC−0.15−NaOH sample means that the monolayer arrangement is reasonable. Thus, NO_3^- (with a dimension of 0.50×0.47 nm[40]) and CO_3^{2-} (0.51×0.48 nm[40]) as well as formamide/water molecules were allowed to enter into the free space in the interlayer gallery.

Formation of the Structure of Bilayered TCAS in the Interlayer. In the XRD pattern of RC−Ag (Figure 4h), a set of basal reflections was observed with d values of 0.36, 0.43, 0.53, 0.72, 1.06, and 2.12 nm corresponding to a minimum periodicity along the c axis equal to 2.12 nm, which means a lamellar structure with 2.12 nm d_{basal} was formed. The gallery height corresponds to the thickness of intercalated TCAS, 1.64 nm (2.12 nm−0.48 nm), being double of that (0.82 nm) in RC−0.02 with a monolayer arrangement of TCAS. Therefore, a bilayered arrangement of TCAS was formed in the sample. No peaks of the separated CO_3^{2-}−LDH phase appeared in the pattern, although high CO_3^{2-} content was found (Table 1). This indicates that CO_3^{2-} exists among the TCAS molecules. The SEM observation on the bilayered TCAS incorporated sample (Figure 3h) found that the particle morphology has no noticeable difference from those of other composites.

Chemical analysis shows that the Ag/TCAS molar ratio is about 1.5 (Table 1), i.e. two TCAS molecules were complexed with three Ag^+ ions, and the average charge of TCAS was decreased to about −4 due to the acidity of $AgNO_3$ introduced. Based on this result, the S_{charge} for TCAS−Ag complex is calculated as $(D^2 \cdot \pi/4)/(4 - 1.5) = 0.38$ nm^2, larger than that of the LDH layer, so that a bilayered arrangement[41,42] of TCAS is formed. Because the S_{charge} value of TCAS−Ag is less than double of that of the LDH sheet, another anion (CO_3^{2-}) can enter the residual space.

It is interesting that different from those of other samples, the d_{basal} value of 2.12 nm was not changed in the water-washing process (Figure 5c−c"). This implies the interactions among layer-TCAS(Ag)-TCAS(Ag)-layer are strong, and the solvent molecules (formamide and water) cannot affect the structure. Because Ag^+ ions coordinate mainly with the bridged S atoms and the phenol oxygen atoms at the bottom-rim,[43] the negative charge concentrates on the upper-rim. The upper-rims of two TCAS adhered to two adjacent LDH sheets, respectively, while their bottom-rims were linked through complexation with three Ag^+ ions. This probably accounts for the formation of a bilayered intercalate, rather than an "up-down" antiparallel arrangement as found for the RC−0.15.

The Structure Models of the Restored Composites. A schematic representation for the formation of the restored composites is proposed (Scheme 2). After the TCAS is added into the colloidal suspension of the osmotically swollen LDH sheets, the interaction between TCAS anions and the layers would be the initial stage of the process, where the area-charge matching takes effect. The upper-rim of TCAS with a higher negative charge density could interact electrostatically with the LDH sheets directly, sandwiched by TCAS molecules i.e. the TCAS orients its cavity axis vertical to the LDH layer with SO_3^- groups anchored to the layer. These interactions, consequently, counteract the repulsion of the sheets, leading to their restoration.

When S_{charge} (TCAS) < S_{charge} (LDH), and the TCAS content is low (Scheme 2a), TCAS molecules are disperse, and their interaction is weak. Thus, a "standard" monolayer structure forms with basal spacing of 1.3 nm. When the TCAS content increases (Scheme 2b), the $\pi-\pi$ stacking interactions between TCAS molecules become strong enough to form a claylike alternating "up-down" antiparallel arrangement in the interlayer, leading to the 1.54 nm d_{basal}. The appearances of only the d_{basal} values of 1.54 and 1.3 nm but not continuous or other variable distances exhibit that the steric characteristics of gallery species can take an important role in the formation of gallery structures. If the charge of TCAS is increased (Scheme 2c), then the electrostatic interaction between TCAS and the sheets becomes strong, resulting in a decrease of d_{basal} to 1.45 nm.

When S_{charge} (TCAS) > S_{charge} (LDH), the bilayer TCAS gallery forms (Scheme 2d). The binding interaction of Ag^+ and TCAS may also play a major role in the formation of the head-to-head configuration.

FT-IR and Thermal Analysis. FT-IR spectra of the samples are given in Figure 2. In the spectra of the composites (Figure 2c−j), the bands at 680 and 444 cm^{-1}, assigned to the Mg(Al)−O stretching vibrations,[23b] and the band at 1044 cm^{-1}, attributed to the S−O bond,[12a] in TCAS were observed. However, the band at 1450 cm^{-1}, assigned to the benzene ring in pure TCAS (Figure 2b), was shifted to 1455 cm^{-1} in the composites. The doublet of 1189 and 1144 cm^{-1} characteristic of $-SO_3$[32] in pure TCAS (Figure 2b) was translated into a broadband at 1173 cm^{-1} in the composites. These indicate the

(40) Xu, Z. P.; Zeng, H. C. *J. Phys. Chem. B* **2001**, *105*, 1743.
(41) Iyi, N.; Kurashima, K.; Fujita, T. *Chem. Mater.* **2002**, *14*, 583.
(42) Costantino, U.; Coletti, N.; Nocchetti, M.; Aloisi, G. G.; Elisei, F. *Langmuir* **1999**, *15*, 4454.
(43) Wu, M.; Yuan, D.; Huang, Y.; Wei, W.; Gao, Q.; Jiang, F.; Hong, M. *Cryst. Growth Des.* **2007**, *7*, 1446.

Scheme 2. Schematic Representation of the Formation and Structure of the Different RC-x Samples

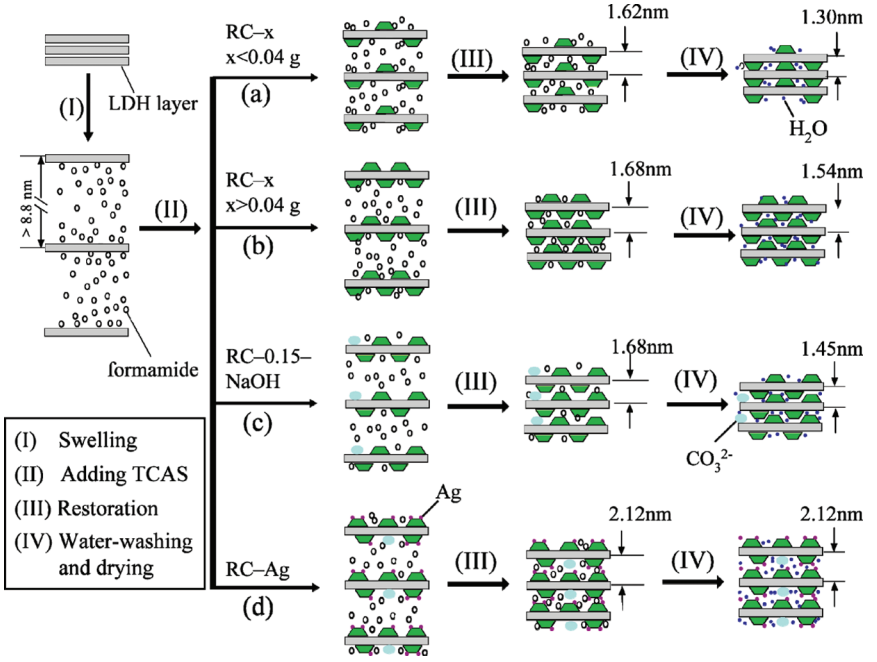

interaction between TCAS and the LDH layer, including the hydrogen-bonding to the hydroxyl groups of the layers. In addition, in RC−Ag, the enhanced band at 1570 cm^{-1}, characteristic of the benzene ring of TCAS, may indicate an interaction between Ag^{+} ions and the phenolic groups at the bottom-rim.

The band at 1384 cm^{-1} is assigned the N−O vibration of NO_3^-, and the band at 1360 cm^{-1} is the C−O vibration of CO_3^{2-}. Their changes of relative intensity show that there were both anions in samples RC−0.01 and RC−0.02, but only CO_3^{2-} was observed from RC−0.04 (Figure 2e), agreeing well with the chemical analysis results for the composites (Table 1).

The TG-DSC curves of pure NO_3^-−LDH, TCAS, and the composites are shown in Figure 6. For the NO_3^-−LDH crystals (Figure 6a), there are two distinct thermal behaviors. Below 170 °C, 6% weight loss is caused by water loss, accompanying one broad endothermic peak at about 60 °C. The 34% weight loss from 170 to 520 °C is because of the dehydration of the brucite-like layers as well as decomposition of the nitrate anions, with three endothermic peaks at around 240, 340, and 450 °C.[44] The thermal behavior of pure TCAS (Figure 6b) was characterized by four steps. The first two weight losses below 385 °C are attributed to the water losses. The losses between 390 and 500 °C, corresponding to two high and strong exothermic peaks at about 430 and 470 °C, result from degradation and combustion of TCAS.

The composites have the TG curves with the similar weight loss steps (Figure 6c−e, at the bottom frame). (1) Below 500 °C, there are three steps, without large endothermic or exothermic peaks except the exothermic

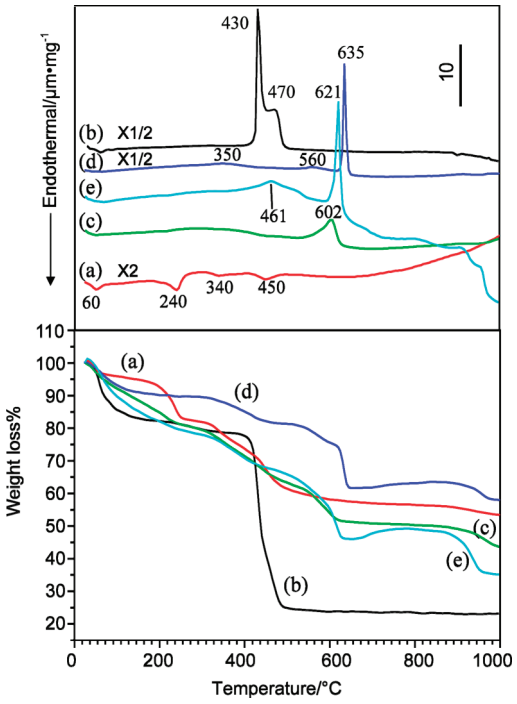

Figure 6. TG-DSC curves of (a) NO_3^-−LDH, (b) TCAS, (c) RC−0.02, (d) RC−0.15, and (e) RC−Ag.

one at 461 °C for RC−Ag. These losses were caused by water release and degradation of partial TCAS. (2) From 500 to 650 °C, two weight losses take place, corresponding to exothermic peaks, at 560 and 635 °C for RC−0.15, at 602 °C for RC−0.02, and at 621 °C for RC−Ag. These results indicate that for the composites, the thermal stability of TCAS was raised by larger than 100 °C. The "up-down" antiparallel arrangement of TCAS in the interlayer shows the largest increase of TCAS decomposition temperature (about 200 °C), indicating the highest thermal stability of the structure. This significant increase

(44) (a) Rives, V. *Inorg. Chem.* **1999**, *38*, 406. (b) Tsai, T.-Y.; Lu, S.-W.; Huang, Y.-P.; Li, F.-S. *J. Phys. Chem. Solids* **2006**, *67*, 938. (c) Li, F.; Zhang, L.; Evans, D. G.; Forano, C.; Duan, X. *Thermochim. Acta* **2004**, *424*, 15.

in thermal stability of TCAS may be a result of the interactions between TCAS and the host layer or the restriction of oxygen diffusion by the presence of the host layers.[45]

Conclusions

By adding TCAS, the osmotically swollen LDH nanosheets were restored to composites with TCAS in the interlayer. This swelling/restoration reaction takes place, and the composites retain the hexagonal morphology of the LDH precursor. TCAS molecules in the interlayer have monolayered, bilayered, and alternating "up-down" antiparallel arrangements, corresponding to basal spacings of 1.30, 2.12, and 1.54 (and 1.45) nm, respectively. The restoration process could be separated into two steps, the electrostatic binding of TCAS to the swollen nanosheets followed by a restacking of the TCAS-sandwiched layers. The area-charge matching can be a predominated factor that controls the arrangement of intercalates in the interlayer. The interaction among TCAS molecules and that between TCAS and the layer may take an important role in the formation of detailed gallery structure, i.e. "standard" monolayered or up−down antiparallel arrangement. The complexation of Ag^+ and TCAS may lead to the formation of a head-to-head bilayered arrangement of TCAS. The decomposition temperature of the intercalated TCAS was heightened by 100 °C than the pure TCAS.

Acknowledgment. This work is supported by the National Science Foundations of China 20671012, 50872012, and 20871018.

Supporting Information Available: Photographs of the colloidal suspension of the LDH in formamide and the sample after TCAS was added and FTIR spectra for the composites during water-washing. This material is available free of charge via the Internet at http://pubs.acs.org.

(45) Wang, J.; Wei, M.; Rao, G. Y.; Evans, D. G.; Duan, X. *J. Solid State Chem.* **2004**, *177*, 366.